Photoinduced electron transfer in a β,β′-pyrrolic fused ferrocene–(zinc porphyrin)–fullerene

David Curiel,[a] Kei Ohkubo,[b] Jeffrey R. Reimers,*[a] Shunichi Fukuzumi*[b] and Maxwell J. Crossley*[a]

Received 19th March 2007, Accepted 25th June 2007
First published as an Advance Article on the web 2nd August 2007
DOI: 10.1039/b704136e

A donor–acceptor linked triad with a short spacer (Fc-ZnP-C_{60}) **1** was designed and synthesised to attain the longest charge-separation lifetime, 630 μs, ever reported for triads at room temperature. The ferrocene electron donor and fullerene electron acceptor of triad **1** are attached to imidazole rings fused to opposite β,β′-pyrrolic positions of the zinc porphyrin. After excitation of the porphyrin, electron transfer to C_{60} occurs within 230 ps, followed by hole transfer to ferrocene after 500 ps to produce the long-lived charge-separated state.

Introduction

Mimicry of the natural photosynthetic process, either in its earlier light harvesting stage or its later charge separation stage, has become a very active area of research during the last decade. Many macromolecular model compounds have been synthesised with the difficult goal of using them in solar energy conversion. In these compounds a difference of potential can be generated by means of a charge-separated state.[1–5] The most common approach for the design of these molecules follows the pattern of donor–bridge–acceptor, in which the charge separation arises from a photoinduced electron transfer between the two ends of the molecule.[1–5] Porphyrins, present in the natural photosynthetic system, represent the most common components in the artificial design. Due to their photophysical properties metalloporphyrins have been predominantly used as electron-donor units.[1–5]

Commonly, porphyrin-based donor–acceptor macromolecules are bridged through the *meso*-position of the porphyrinic ring. Recently, we reported very long lived charge-shift states in triads and tetrads with zinc(II) porphyrin as donors and gold(III) porphyrins as acceptor components in which the porphyrins are bridged through β,β′-pyrrolic positions rather than *meso*-positions;[6] these compounds also represent the closest chemical models for the arrangement of the chromophores in the photosynthetic reaction centre.[6] We have also shown that a β,β′-pyrrolic linkage improves the lifetime of the charge-separated state in porphyrin–fullerene dyads, and in particular dyad **2**, when compared to systems with a similar donor–acceptor distance but linked through the *meso*-position.[7] In this paper we report the synthesis and investigate the photophysical properties of the triad **1** which has β,β′-pyrrolic linkages between the components and also makes use of a fullerene as the acceptor unit.

The incorporation of C_{60} fullerenes as electron-acceptor components has become increasingly widespread due to their excellent structural, electrochemical and photochemical properties that enables stabilisation of charge-separated states by decreasing the rate of charge recombination.[8–12] Several factors such as solvent polarity,[13] donor–acceptor distance and the nature of the bridge[14] have been thoroughly analysed in the porphyrin–fullerene systems in order to get a better understanding of the electron-transfer process taking place in solution. Another well known strategy employed to increase the lifetime of the charge-separated state involves a sequential electron transfer to attain the final charge-separated state.[1–5] With the charges located further apart than in basic dyads, the ion pair resulting from a multi-step electron transfer should slow down the charge-recombination rate.

In the molecular triad **1**, a ferrocene unit and a fullerene unit are linked at opposite sides of the porphyrin macrocycle through its β,β′-pyrrolic positions by means of fused imidazole rings; the expectation being that this arrangement of chromophores should lead to a long-lived charge-separated state. Indeed, this was found to be the case. Additionally, electrochemical, photochemical and computational studies have been carried out to determine the mechanism of the electron transfer occurring across the molecule.

Experimental

General

Ultraviolet-visible spectra were recorded on a Cary 5E UV-Vis-NIR spectrophotometer using purified benzonitrile (PhCN) as solvent. ^{1}H NMR spectra were recorded on a Bruker DPX-400 (400 MHz) spectrometer. Samples were dissolved in deacidified deuteriochloroform ($CDCl_3$) and the chloroform peak at 7.26 ppm used as an internal reference.

High resolution electrospray ionization Fourier transform ion cyclotron resonance (HR-ESI-FT/ICR) spectra were

[a] *School of Chemistry, The University of Sydney, NSW 2006, Australia. E-mail: m.crossley@chem.usyd.edu.au; Fax: +612 9351 6650; Tel: +612 9351 2751*
[b] *Department of Material and Life Science, Graduate School of Engineering, Osaka University, SORST, Japan Science and Technology Agency, Suita, Osaka 565-0871, Japan. E-mail: fukuzumi@chem.eng.osaka-u.ac.jp; Tel: +816 6879 7368*

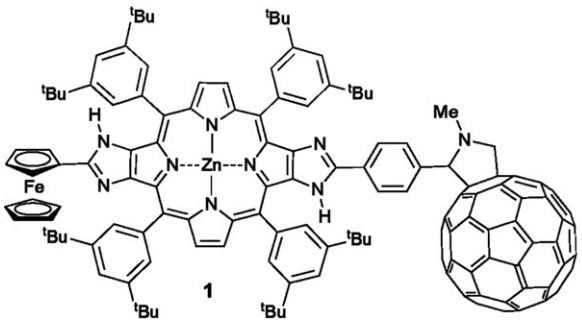

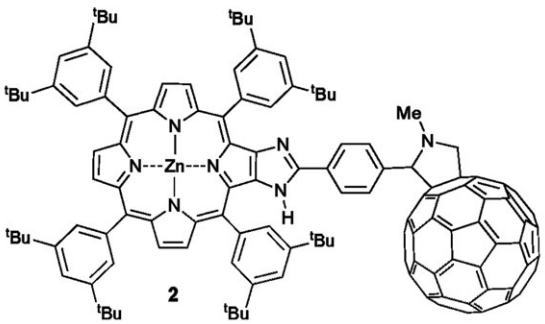

acquired at the School of Chemistry, The University of New South Wales on a Bruker Daltonics BioAPEX II FT/ICR mass spectrometer equipped with a 7 T MAGNEX superconducting magnet and an Analytica external ESI source. Electrospray ionization high resolution mass spectrometry (ES-MS) were recorded on either a VG Quattro II triple quadrupole mass spectrometer at the Research School of Chemistry, Australian National University.

Steady-state absorption spectra in the visible and near-IR regions were measured on a Shimadzu UV-3100PC.

Materials

All commercial solvents were routinely distilled prior to use. Solvent mixture proportions are given by volume ratios. Light petroleum refers to the fraction with bp 60–80 °C.

Tetrabutylammonium hexafluorophosphate used as a supporting electrolyte for the electrochemical measurements was obtained from Tokyo Kasei Organic Chemicals. PhCN was purchased from Wako Pure Chemical Ind., Ltd, and purified by successive distillation over P_2O_5.

Synthesis

Ferrocene–(zinc porphyrin)–fullerene triad 1. Porphyrin–tetraone **3** (150 mg, 0.13 mmol), ferrocene–carboxaldehyde (24 mg, 0.11 mmol) and ammonium acetate (0.5 g, 6.4 mmol) were stirred in a $CHCl_3$: AcOH (9 : 1) mixture at reflux temperature for 6 h. The reaction was then allowed to cool to room temperature and solvents were evaporated under reduced pressure. The resulting crude product was chromatographed over silica gel (DCM–AcOEt, 20 : 1) and this yielded ferrocene–porphyrin–dione **4** as a purple solid (79 mg, 45% yield), mp >300 °C. ^{1}H-NMR ($CDCl_3$, ppm): −2.38 (s, 1H), −2.19 (s, 1H), 1.47 (s, 36H), 1.55 (s, 36H), 4.06 (s, 5H), 4.59 (t, J = 1.8 Hz, 2H), 4.66 (t, J = 1.8 Hz, 2H), 7.75–8.05 (m, 13H), 8.66 (b, 2H), 8.79 (b, 2H). ES-MS (m/z): 1317.80 (M^+), 1318.67 (M^+ + 1).

The foregoing ferrocene–porphyrin–dione **4** (50 mg, 0.04 mmol) was stirred in the presence of excess of terephthaldehyde (50 mg, 0.4 mmol) and ammonium acetate (0.42 g, 1.9 mmol) in a mixture of $CHCl_3$: AcOH (9 : 1) at reflux temperature for 6 h. After allowing the mixture to cool to room temperature the solvents were evaporated under reduced pressure. Without further purification, the resulting crude product was dissolved in a mixture of CH_2Cl_2 : MeOH and stirred at reflux temperature in the presence of $Zn(AcO)_2 \cdot 2H_2O$ (50 mg, 0.23 mmol) for 4 h. When the reaction had cooled to room temperature, the solvents were evaporated under reduced pressure. Liquid chromatography of the crude product through a silica gel column, eluting with CH_2Cl_2–AcOEt (20 : 1) and crystallisation from a mixture of CH_2Cl_2–MeOH of the product isolated by evaporation of the main band gave the ferrocene–porphyrinoimidazole–phenylaldehyde **5** as a purple microcrystalline solid (36 mg, 62% overall yield for the two steps), mp > 300 °C. ^{1}H-NMR ($CDCl_3$, ppm): 1.57 (bs, 72H), 4.11 (s, 5H), 4.40 (t, J = 1.8 Hz, 2H), 4.70 (t, J = 1.8 Hz, 2H), 7.91–8.17 (m, 17H), 8.61 (s, 1H) 9.07–9.15 (m, 4H), 10.06 (s, 1H). ES-MS (m/z): 1495.73 (M^+).

The foregoing aldehyde **5** (33 mg, 0.022 mmol), fullerene (24 mg, 0.033 mmol) and *N*-methylglycine (8 mg, 0.088 mol), were heated in toluene (25 ml) at reflux for 6 h. The solvent was then evaporated under reduced pressure and the crude product was chromatographed over silica gel (ethyl acetate, 0 to 5% in toluene). Ferrocene–(zinc porphyrin)–fullerene *triad* **1** was isolated as an analytically pure purple solid (35.5 mg, 73% yield), mp > 300 °C. UV-Vis (PhCN); λ (cm^{-1}) (ε (cm^{-1} M^{-1})): 434 (2.83×10^5), 524 (1.03×10^4), 558 (1.57×10^4), 603 (3.08×10^4); ^{1}H-NMR ($CDCl_3$, ppm): 1.55 (bs, 72H), 2.85 (s, 3H), 4.09 (s, 5H), 4.18 (d, J = 9.6 Hz, 1H), 4.38 (s 2H), 4.70 (s, 2H), 4.86–4.92 (m, 2H), 7.80–7.87 (m, 4H), 7.95–8.24 (m, 13H), 8.49 (s, 1H) 9.02–9.15 (m, 4H); HR-ESI-FT/ICR (m/z): Found: $[M + 2H]^{2+}$ 1121.8816. $[C_{157}H_{109}N_9FeZn + 2H]^{2+}$ requires: 1121.8817.

Compounds **2**, **6** and **7** were prepared in other work in our laboratory.[15]

Spectral measurements

Femtosecond transient absorption spectroscopy experiments were conducted using an ultrafast source: Integra-C (Quantronix Corp.), an optical parametric amplifier: TOPAS (Light Conversion Ltd.) and a commercially available optical detection system: Helios provided by Ultrafast Systems LLC. The source for the pump and probe pulses were derived from the fundamental output of Integra-C (780 nm, 2 mJ $pulse^{-1}$ and fwhm = 130 fs) at a repetition rate of 1 kHz. 75% of the fundamental output of the laser was introduced into TOPAS which has optical frequency mixers resulting in a tunable range from 285 nm to 1660 nm, while the rest of the output was used for white light generation. Prior to generating the probe continuum, a variable neutral density filter was inserted in the path in order to generate stable continuum, then the laser pulse was fed to a delay line that provides an experimental

time window of 3.2 ns with a maximum step resolution of 7 fs. In our experiments, a wavelength between 350 nm to 450 nm of TOPAS output, which is the fourth harmonic of signal or idler pulses, was chosen as the pump beam. As this TOPAS output consists of not only desirable wavelength but also unnecessary wavelengths, the latter was deviated using a wedge prism with a wedge angle of 18°. The desirable beam was irradiated at the sample cell with a spot size of 1 mm diameter where it was merged with the white probe pulse in a close angle (<10°). The probe beam after passing through the 2 mm sample cell was focused on a fiber optic cable that was connected to a CCD spectrograph for recording the time-resolved spectra (410–800 nm). Typically, 2500 excitation pulses were averaged for 5 s to obtain the transient spectrum at a set delay time. Kinetic traces at appropriate wavelengths were assembled from the time-resolved spectral data. All measurements were conducted at room temperature, 295 K.

For nanosecond laser flash photolysis experiments, a deaerated PhCN solutions (pH 7.0) of dyad or triad was excited by a Panther OPO pumped by Nd : YAG laser (Continuum, SLII-10, 4–6 ns fwhm) at λ = 430 nm with a power of 5 mJ pulse^{-1}. The photochemical reactions were monitored by continuous exposure to a Xe-lamp (150 W) as a probe light and a photomultiplier tube (Hamamatsu 2949) as a detector. For transient absorption spectra in the near-IR region (800–1200 nm), monitoring light from a pulsed Xe-lamp was detected with a Ge-avalanche photodiode (Hamamatsu Photonics, B2834). The transient spectra were recorded using fresh solutions in each laser excitation. All experiments were performed at 298 K.

The quantum yields were measured using the comparative method. In particular, the strong monofunctionalized fullerene triplet–triplet absorption ($\varepsilon_{700\ nm}$ = 16 100 M^{-1} cm^{-1}; $\Phi_{TRIPLET}$ = 0.98) served as a probe to obtain the quantum yield for the CS state, especially for the monofunctionalized fullerene π-radical anion ($\varepsilon_{1000\ nm}$ = 4700 M^{-1} cm^{-1}).[16]

Electrochemical measurements

The cyclic voltammetry measurements were performed on a BAS 50W electrochemical analyzer in a deaerated PhCN solution containing 0.10 M *n*-Bu_4NPF_6 as a supporting electrolyte at 298 K (10 mV s^{-1}). The platinum working electrode was polished with BAS polishing alumina suspension and rinsed with acetone before use. The counter electrode was a platinum wire. The measured potentials were recorded with respect to an $Ag/AgNO_3$ (0.01 M) reference electrode. Ferrocene/ferricenium was used as an external standard.

Theoretical calculations

Density-functional theory (DFT) geometry optimizations for the final charge-transfer state were performed with the B3LYP functional[17,18] with the LANL2DZ basis[19] for Zn and Fe and the 3-21G basis set[20] for the remaining atoms. All calculations were performed using a self-consistent reaction field set to model solvation in PhCN; all porphyrin *meso* Ar substituents were replaced with hydrogen.

Results and discussion

The synthesis of triad **1** was achieved by sequential fusion of functionalized imidazole rings to the porphyrin pyrrolic 2,3,12,13-positions following the method developed by Crossley and McDonald.[15] Thus, reaction of tetraone[21] **3** with ferrocenecarboxaldehyde in the presence of ammonium acetate in a refluxing mixture of $CHCl_3$: AcOH (5 : 1), followed by a similar condensation of the resultant dione **4** with terephthaldehyde and addition of zinc(II) gave **5** in good overall yield (Scheme 1). Finally, the incorporation of fullerene into the structure was accomplished through the azomethine ylide insertion mediated by sarcosine between C_{60} and **5**.

Triad **1** was isolated by liquid chromatography in 73% yield and was characterised by the usual spectroscopic techniques. Due to slow N–H tautomerization of the imidazole rings, on the ^{1}H-NMR timescale at room temperature, a mixture of geometric isomers could be detected in the case of dione **4**.

Electrochemical studies were carried out to estimate the effect of the fused imidazole rings on the redox properties of the porphyrin macrocycle (Table 1). Comparing the first oxidation potential of bis-(imidazolo)porphyrin **6** to that of [5,10-15,20-tetrakis(3,5-di-*tert*-butylphenyl)porphyrinato]-zinc(II) **7**, a small electron-releasing effect from the imidazole

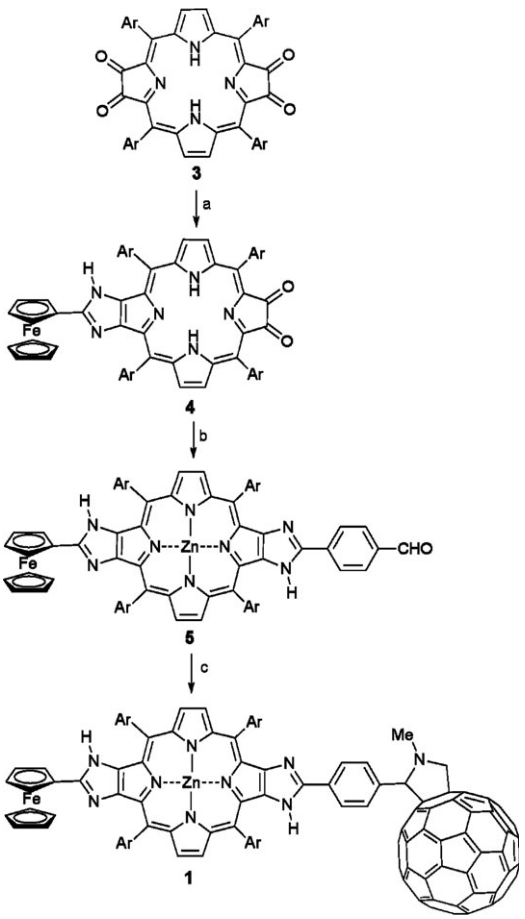

Scheme 1 (a) Ferrocenecarboxaldehyde, NH_4OAc, $CHCl_3$: AcOH (5 : 1), reflux (45%); (b) 1. $Zn(AcO)_2 \cdot 2H_2O$, CH_2Cl_2 : MeOH (3 : 1), reflux; 2. Terephthaldehyde, NH_4OAc, $CHCl_3$: AcOH (5 : 1), reflux (62%); (c) Sarcosine, fullerene, toluene, reflux (73%). Ar = 3,5-di-*tert*-butylphenyl.

Table 1 Electrochemical potentials (mV) in *o*-dichlorobenzene and PhCN determined by cyclic voltammetry,[a] as well as free energy changes ΔG (eV) for electron-transfer processes in *o*-dichlorobenzene and PhCN calculated from the electrochemical potentials after correction for the Coulomb interaction between the charges in the triad[b]

Solvent	Compound	Half-wave potentials			Free energy increments			
		$ZnP^{\bullet+}/ZnP$	Fc^{+}/Fc	$C_{60}/C_{60}^{\bullet-}$	ΔG_{CS1}	ΔG_{CR1}	ΔG_{CS2}	ΔG_{CR2}
o-Dichlorobenzene	**7**	788						
	6	773						
	1	774	662	−592	−0.79	−1.27	−0.08	−1.19
PhCN	**6**	758						
	1	801	598	−530	−0.75	−1.30	−0.19	−1.11

[a] [Porphyrin] = 8×10^{-4} M, $TBAClO_4$ (0.1 M), T = 25 °C, scan rate: 100 mV s^{-1}, reference: Ag/AgCl. [b] $\Delta G_{CR1} = E_{1/2}(C_{60}\ \text{red.}) - E_{1/2}(ZnP\ \text{ox.}) + 1/\varepsilon_0 R_{C60\text{–}ZnP}$ is for charge recombination from $Fc\text{-}ZnP^{\bullet+}\text{-}C_{60}^{\bullet-}$; $\Delta G_{CS1} = -\Delta G_{CR1} - \Delta E_{0\text{–}0}$ is the driving force for primary charge separation where $\Delta E_{0\text{–}0}$ is the energy of the lowest excited state calculated as the average of the energy of the (0–0) band in the absorption and the emission spectra; $\Delta G_{CS2} = E_{1/2}(Fc\ \text{ox.}) - E_{1/2}(ZnP\ \text{ox.}) + 1/\varepsilon_0 R_{C60\text{–}ZnP} - 1/\varepsilon_0 R_{C60\text{–}Fc}$ is the driving force for secondary charge separation; and $\Delta G_{CR2} = \Delta G_{CR1} - \Delta G_{CS2} = E_{1/2}(C_{60}\ \text{red.}) - E_{1/2}(Fc\ \text{ox.}) + 1/\varepsilon_0 R_{C60\text{–}Fc}$ is the driving force for the charge recombination from the fully charged separated state. The parameters used are: ε_0 = 25.2 for PhCN and 10.1 for *o*-dichlorobenzene and, from the DFT calculations, $R_{C60\text{–}ZnP}$ = 15 Å and $R_{C60\text{–}Fc}$ = 23 Å.

rings can be detected. Within the accuracy limits of cyclic voltammetry, a cathodic shift (15 mV) of the half wave potential, $E_{1/2}(ZnP^{\bullet+}/ZnP)$, of **6** in *o*-dichorobenzene is estimated. Little change in the porphyrin-centred potential of triad **1** compared to the model compound **6** was detected in *o*-dichlorobenzene but a shift of 43 mV was observed in PhCN (Table 1), suggesting a significant interaction between the ferrocene HOMO and the porphyrin.

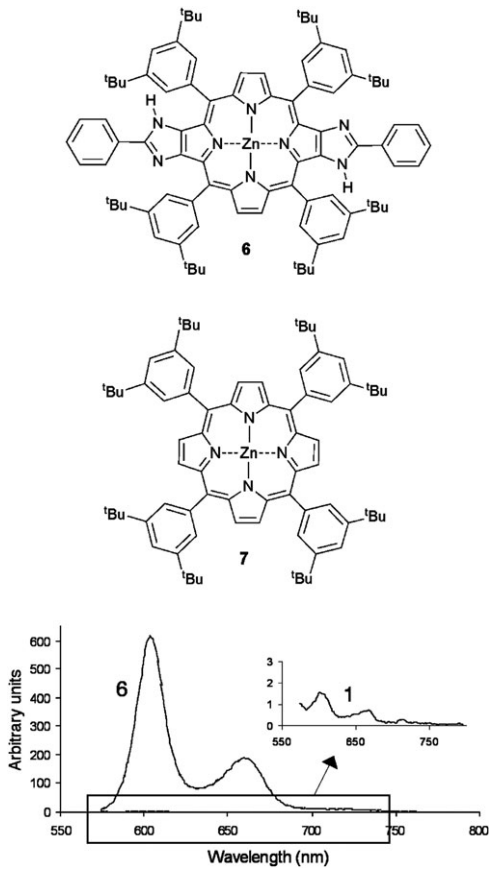

Fig. 1 Emission spectra (λ_{exc} = 552 nm) of **6** and **1** (inset) (3×10^{-6} M) in dichlorobenzene.

The shape and maxima of the bands seen in the absorption spectra of the triad **1** in *o*-dichlorobenzene and PhCN solutions can be interpreted as a superposition of the absorption spectra of each of the individual components. This indicates that the porphyrin orbitals giving rise to these absorptions are at most slightly perturbed by the donor and acceptor groups. Conversely, the emission spectrum of **1**, using λ_{ex} = 551 nm for the selective excitation of the porphyrin component showed a dramatic quenching of the fluorescence when compared with the control compound **6** (Fig. 1). This clearly indicates the occurrence of a new electronic process amongst the excited state of the triad **1**.

Shown in Fig. 2 are time-resolved transient absorption spectra of the dyad (ZnP-C_{60}) **2** observed by femtosecond laser flash photolysis in deaerated PhCN. These decay *via* two steps up to 2000 ps. The fast decay component of absorbance at 470 nm in Fig. 3(a) with the rate constant of 2.8×10^{11} s^{-1} corresponds to the conversion of the excited Soret states of the ZnP component formed by femtosecond laser excitation at 355 nm to the lowest *Q*-band (S_1) state, because the decay rate constant agrees with that obtained from the fluorescence lifetime of the Soret bands of ZnP.[22] The much slower decay of absorbance at 626 nm with the rate constant of 5.8×10^9 s^{-1} in Fig. 3b may correspond to electron transfer from the lowest *Q* band of the ZnP component to the C_{60} component, because the fluorescence of the *Q* state of the ZnP component is efficiently quenched in ZnP-C_{60}.[7]

Similar transient absorption spectra are observed for the triad (**1**: Fc-ZnP-C_{60}) as shown in Fig. 4.

The conversion of the Soret states to the lowest *Q* state monitored by decay of absorbance at 470 nm in Fig. 5a, which is similar to that in Fig. 3a, is followed by electron transfer from the S_1 state of the ZnP unit to the C_{60} unit, as shown in Fig. 5b. The rate constant of the conversion of the Soret states to the S_1 state (1.0×10^{11} s^{-1}) and that of the electron transfer (4.3×10^9 s^{-1}) for the triad **1** agree with those determined for the dyad **2**. The electron-transfer rate constant is comparable with that reported for a similar ZnP-C_{60} dyad in benzonitrile (9.5×10^9 s^{-1}).[11] The notable difference between the dyad **2** and the triad **1** is the slow disappearance of absorbances at 470 nm and 700 nm due to the $ZnP^{\bullet+}$ component of **1** in the

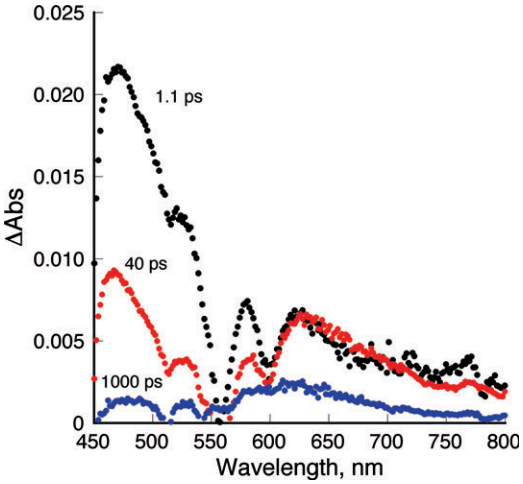

Fig. 2 Transient absorption spectra of ZnP-C_{60} **2** taken at 1.1 ps, 40 ps and 1000 ps after fs laser pulse irradiation at 355 nm in PhCN at 298 K.

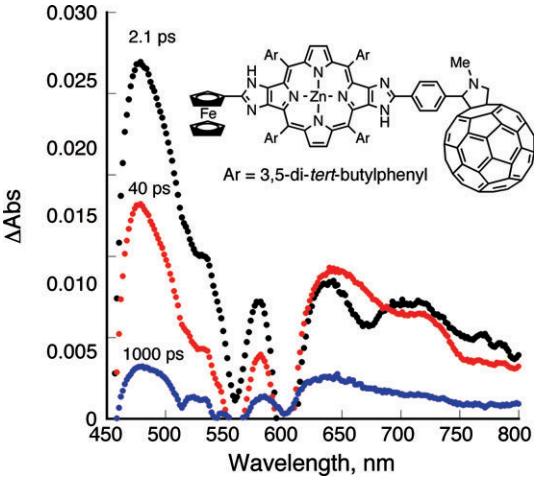

Fig. 4 Transient absorption spectra of Fc-ZnP-C_{60} **1** taken at 2.1 ps, 40 ps and 1000 ps after femtosecond laser pulse irradiation at 355 nm in PhCN at 298 K.

nanosecond timescale (Fig. 5b) as compared with the existence of the residual absorbance at 626 nm due to the $ZnP^{\bullet+}$ component in the dyad (Fig. 3b). This indicates the occurrence of subsequent electron transfer from the Fc component to the $ZnP^{\bullet+}$ component in the triad **1** to afford the final charge-separated state (Fc^{+}-ZnP-$C_{60}^{\bullet-}$). The electron-transfer rate constant is estimated as 2×10^{9} s^{-1} from the decay of absorbance at 470 nm at the prolonged delay time up to 1.5 ns (Fig. 5b). This rate is much faster than the back electron transfer from the $C_{60}^{\bullet-}$ component to the $ZnP^{\bullet+}$ component in the dyad **2** (4.3×10^{3} s^{-1}),[7] leading to formation of the final charge-separated state (Fc^{+}-ZnP-$C_{60}^{\bullet-}$).

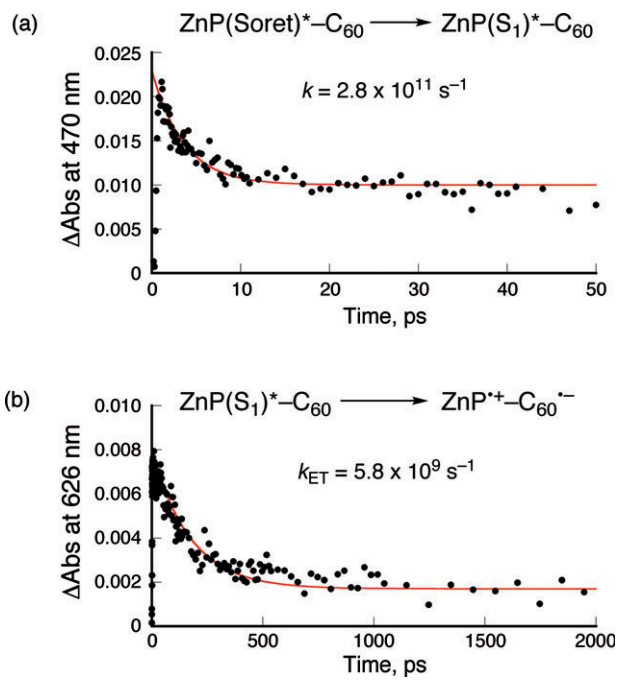

Fig. 3 Decay profiles of absorbance of ZnP-C_{60} **2** at (a) 470 nm and (b) 626 nm.

The formation of the final charge-separated state (Fc^{+}-ZnP-$C_{60}^{\bullet-}$) from **1** is confirmed by the nanosecond laser flash photolysis. Fig. 6 shows the transient absorption spectra in the visible and NIR region. The visible absorption band at 500 nm and the NIR band at 1050 nm are diagnostic of the radical anion of C_{60} derivatives.[16,23] It should be noted that the absorption band at 650 nm due to the $ZnP^{\bullet+}$ component is absent in Fig. 6. With regard to the Fc^{+} component, the weak absorption features of the ferricenium ion (λ_{max} = 620 nm, ε_{max} = 330 dm^3 mol^{-1} cm^{-1})[24] have precluded its detection in the transient absorption spectrum.

From the decay time profile of absorbance at 490 nm the lifetime of the CS state is determined as 630 μs at 298 K. This is the longest CS lifetime ever reported for a triad at room temperature. The energy diagram of Fc-ZnP-C_{60} **1** is

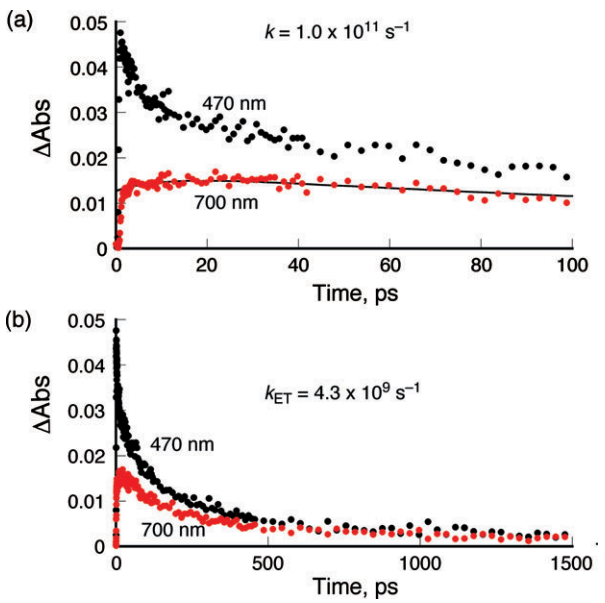

Fig. 5 Decay time profiles of absorbance of Fc-ZnP-C_{60} **1** upon femtosecond laser pulse irradiation observed at 470 nm and 700 nm in the 1–100 ps range and in the 1–1500 ps range.

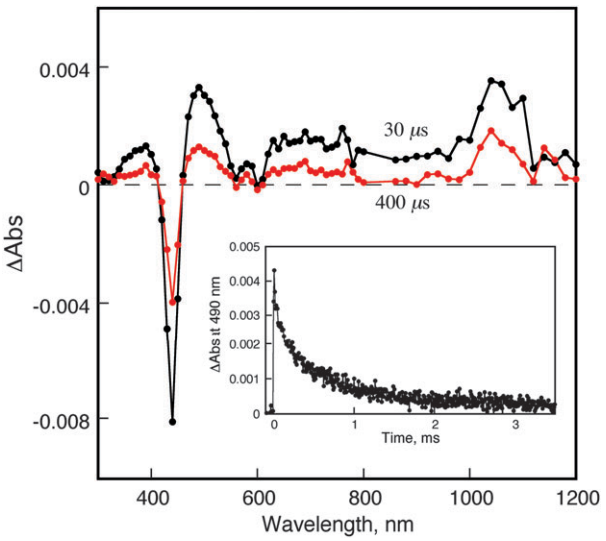

Fig. 6 Transient absorption spectra of Fc-ZnP-C_{60} **1** taken at 30 μs and 400 μs after nanosecond laser pulse irradiation at 430 nm in PhCN at 298 K. Decay profile of absorbance at 490 nm is shown in the inset.

summarized in Scheme 2 with the lifetime of each transient species in the photoinduced electron-transfer reaction.

It is particularly noteworthy that the CS lifetime (630 μs) of Fc^+-ZnP-$C_{60}^{\bullet-}$ is much longer than the lifetime (8 μs) of a similar triad linked by a longer amide linkage, Fc^+-NHCO-ZnP-CONH–$C_{60}^{\bullet-}$ (Fig. 7).

According to the rate equation for non-adiabatic electron transfer,[25]

$$k = \left(\frac{4\pi^3}{h^2\lambda k_\beta T}\right)^{1/2} V^2 e^{-\Delta G^+/k_\beta T} \text{ with } \Delta G^+ = \frac{(\lambda + \Delta G_0)^2}{4\lambda},$$

the rate constant of electron transfer k with the same driving force ($-\Delta G_0$) depends on the electronic coupling term (V) and the total reorganization energy (λ) of electron transfer. Naively, the shorter donor–acceptor distance (R) should give a larger V and smaller λ; while the enhanced coupling should accelerate electron transfer, the reduced λ for a system in the Marcus inverted region[25] ($\lambda < -\Delta G_0$) should slow it.[26] An indication of the rate retardation expected from the later effect can be obtained using the Marcus approximation to the outer-

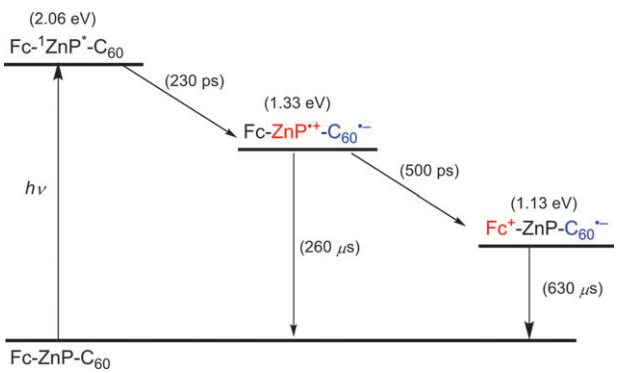

Scheme 2 Energy diagram of Fc-ZnP-C_{60} **1** and the lifetime of each transient species in PhCN; the 260 μs lifetime of the first CS state is estimated from the known lifetime of the CS state of **2**.[7]

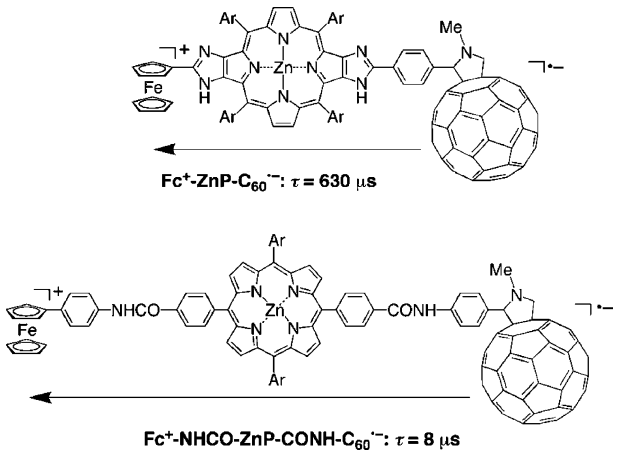

Fig. 7 Comparison of the CS lifetime (τ) between Fc^+-ZnP-$C_{60}^{\bullet-}$ derived from triad **1** and Fc^+-NHCO-ZnP-CONH-$C_{60}^{\bullet-}$.[16]

sphere solvent contribution to the reorganization energy[27]

$$\lambda_o = \frac{1}{2}\left(\frac{1}{R_+} + \frac{1}{R_-} - \frac{2}{R}\right)\left(\frac{1}{\varepsilon_\infty} - \frac{1}{\varepsilon_0}\right) \times 14.4 \quad \text{eV}$$

where the donor and acceptor radii, R_+ and R_-, respectively, are in Å, as is the centre–centre separation R. For PhCN solvent, the static and high-frequency dielectric constants are $\varepsilon_0 = 25.2$ and $\varepsilon_\infty = 2.319$, respectively, and the radii determined from the van der Waals volumes are $R_+ = 3.3$ Å and $R_- = 5.0$ Å. This leads to estimated reorganization energies of $\lambda \sim \lambda_o = 1.25$ eV for charge recombination in Fc^+-NHCO-ZnP-CONH-$C_{60}^{\bullet-}$, close to the observed values[16,23] of 1.09 eV, and 1.16 eV in Fc^+-ZnP-$C_{60}^{\bullet-}$. As a result, a net slowing of the charge recombination rate of just 4% is predicted, much short of the observed factor of 80.

These calculations are based on the assumption that the charges are localized on the donor and acceptor groups. DFT calculations of the structure of the two triads reveal that Fc-ZnP-C_{60} **1** has a conjugated planar linkage extending from the ferrocene ring to the phenyl group that attaches the C_{60} unit, while an extended series of steric interactions forces each successive inter-ring junction in Fc-NHCO-ZnP-CONH-C_{60} to be non-planar. As a result, the highest-occupied molecular orbitals (HOMOs) shown in Fig. 8 are qualitatively different, with that for Fc-NHCO-ZnP-CONH-C_{60} being 88% localized on the ferrocene whilst that for Fc-ZnP-C_{60} **1** is essentially delocalized over the ferrocene (56%) and the porphyrin. When this change of nature of the donor is taken into account, the donor radius becomes $R_+ = 5.1$ Å while the donor–acceptor effective distance becomes $R = 18$ Å. These values result in a calculated solvent reorganization energy $\lambda_o = 0.80$ eV; this is 0.36 eV less than that obtained for a ferrocene-localized charge. Such a change would have a pronounced effect on reducing the rate constant for charge recombination. The observed slow charge-recombination rate from the charge-separated state of Fc-ZnP-C_{60} **1** probably arises from partial cancellation of two effects: the rate reduction stemming from this change in λ, and the rate enhancement due to increased coupling V that arises from the orbital delocalization. Further

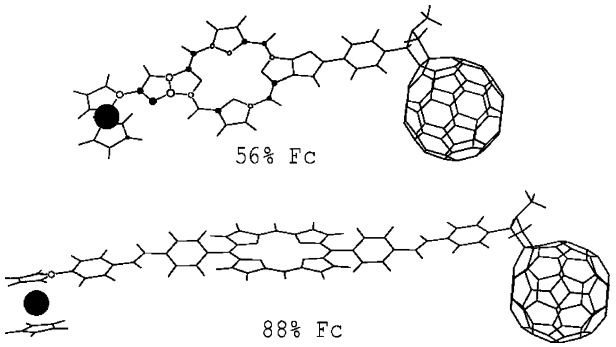

Fig. 8 The calculated structures and HOMO orbitals for Fc-ZnP-C_{60} (upper) and Fc-NHCO-ZnP-CONH-C_{60} (lower), along with their percentage localization on ferrocene (Fc).

studies are underway in order to properly quantify both effects using *a priori* calculation methods.

Conclusions

We have designed and synthesized a donor–acceptor linked triad with a short spacer (Fc-ZnP-C_{60}) **1** to attain the longest CS lifetime, 630 μs, ever reported for a triad at room temperature. Bridge planarity leading to extended π-electron conjugation is most likely responsible for the long lifetime, with donor charge delocalization acting to reduce the reorganization energy, dramatically slowing the charge-recombination reaction. Control of extended delocalization thus offers a new motif through which charge-transfer reactions may be controlled by subtle chemical variations.

Acknowledgements

This work was supported by a Discovery Research Grant (DP0208776) to M. J. C. and J. R. R. from the Australian Research Council. This work was partially supported by a Grant-in-Aid (Nos. 16205020 and 17750039) from the Ministry of Education, Culture, Sports, Science and Technology, Japan. We thank the Australian Partnership on Advanced Computing (APAC) for the provision of computer resources.

References

1 (*a*) G. Steinberg-Yfrach, J.-L. Rigaud, E. N. Durantini, A. L. Moore, D. Gust and T. A. Moore, *Nature*, 1998, **392**, 479; (*b*) G. Steinberg-Yfrach, J.-L. Rigaud, E. N. Durantini, A. L. Moore, D. Gust and T. A. Moore, *Nature*, 1997, **385**, 239.
2 (*a*) D. Gust and T. A. Moore, in *The Porphyrin Handbook*, ed. K. M. Kadish, K. M. Smith and R. Guilard, Academic Press, San Diego, CA, 2000, vol. 8, pp. 153–190; (*b*) D. Gust, T. A. Moore and A. L. Moore, *Acc. Chem. Res.*, 2001, **34**, 40; (*c*) D. Gust, T. A. Moore and A. L. Moore, in *Electron Transfer in Chemistry*, ed. V. Balzani, Wiley-VCH, Weinheim, 2001, vol. 3, pp. 272–336.
3 (*a*) S. Fukuzumi and D. M. Guldi, in *Electron Transfer in Chemistry*, ed. V. Balzani, Wiley-VCH, Weinheim, 2001, vol. 2, pp. 270–337; (*b*) S. Fukuzumi, *Org. Biomol. Chem.*, 2003, **1**, 609.
4 (*a*) A. Osuka, N. Mataga and T. Okada, *Pure Appl. Chem.*, 1997, **69**, 797; (*b*) M. R. Wasielewski, *Chem. Rev.*, 1992, **92**, 435.
5 (*a*) K. D. Jordan and M. N. Paddon-Row, *Chem. Rev.*, 1992, **92**, 395; (*b*) M. N. Paddon-Row, *Acc. Chem. Res.*, 1994, **27**, 18.
6 (*a*) M. J. Crossley, P. J. Sintic, J. A. Hutchison and K. P. Ghiggino, *Org. Biomol. Chem.*, 2005, **3**, 852–865; (*b*) K. Ohkubo, P. J. Sintic, N. V. Tkachenko, H. Lemmetyinen, W. E. Z. Ou, J. Shao, K. M. Kadish, M. J. Crossley and S. Fukuzumi, *Chem. Phys.*, 2006, **326**, 3.
7 Y. Kashiwagi, K. Ohkubo, J. A. McDonald, I. M. Blake, M. J. Crossley, Y. Araki, O. Ito, H. Imahori and S. Fukuzumi, *Org. Lett.*, 2003, **5**, 2719.
8 S. Fukuzumi and H. Imahori, in *Electron Transfer in Chemistry*, ed. V. Balzani, Wiley-VCH, Weinheim, 2001, vol. 2, pp. 927–975.
9 (*a*) D. M. Guldi and S. Fukuzumi, in *Fullerenes: From Synthesis to Optoelectronic Properties*, ed. D. M. Guldi and N. Martin, Kluwer, Dordrecht, 2003, pp. 237–265; (*b*) D. M. Guldi, *Phys. Chem. Chem. Phys.*, 2007, **9**, 1400; (*c*) T. M. Figueira-Duarte, A. Gégout and J.-F. Nierengarten, *Chem. Commun.*, 2007, 109.
10 F. D'Souza and O. Ito, *Coord. Chem. Rev.*, 2005, **249**, 1410.
11 Y. Kobori, S. Yamaguchi, K. Akiyama, S. Tero-Kubota, H. Imahori, S. Fukuzumi and J. R. Norris, Jr, *Proc. Natl. Acad. Sci. U. S. A.*, 2005, **102**, 10017.
12 (*a*) F. D'Souza, M. R. El-Khouly, S. Gadde, M. E. Zandler, A. L. McCarty, Y. Araki and O. Ito, *Tetrahedron*, 2006, **62**, 1967; (*b*) K. Ohkubo, H. Kotani, J. Shao, Z. Ou, K. M. Kadish, G. Li, R. K. Pandey, M. Fujitsuka, O. Ito, H. Imahori and S. Fukuzumi, *Angew. Chem., Int. Ed.*, 2004, **43**, 853.
13 H. Imahori, M. E. El-Khouly, M. Fujitsuka, O. Ito, Y. Sakata and S. Fukuzumi, *J. Phys. Chem. A*, 2001, **105**, 325.
14 H. Imahori, K. Tamaki, Y. Araki, T. Hasobe, O. Ito, A. Shimomura, S. Kundu, T. Okada, Y. Sakata and S. Fukuzumi, *J. Phys. Chem. A*, 2002, **106**, 2803.
15 M. J. Crossley and J. A. McDonald, *J. Chem. Soc., Perkin Trans. 1*, 1999, 2429.
16 H. Imahori, K. Tamaki, D. M. Guldi, C. Luo, M. Fujitsuka, O. Ito, Y. Sakata and S. Fukuzumi, *J. Am. Chem. Soc.*, 2001, **123**, 2607.
17 A. D. Becke, *J. Chem. Phys.*, 1993, **98**, 5648.
18 C. Lee, W. Yang and R. G. Parr, *Phys. Rev. B: Condens. Matter Mater. Phys.*, 1988, **37**, 785.
19 P. J. Hay and W. R. Wadt, *J. Chem. Phys.*, 1985, **82**, 270.
20 W. J. Hehre, L. Radom, P. v. R. Schleyer and J. A. Pople, *Ab initio Molecular Orbital Theory*, Wiley, New York, 1986.
21 M. J. Crossley, L. J. Govenlock and J. K. Prashar, *J. Chem. Soc., Chem. Commun.*, 1995, 2379.
22 (*a*) N. Mataga, H. Chosrowjan, Y. Shibata, N. Yoshida, A. Osuka, T. Kikuzawa and T. Okada, *J. Am. Chem. Soc.*, 2001, **123**, 12422; (*b*) N. Mataga, Y. Shibata, H. Chosrowjan, N. Yoshida and A. Osuka, *J. Phys. Chem. B*, 2004, **104**, 4001.
23 H. Imahori, D. M. Guldi, K. Tamaki, Y. Yoshida, C. Luo, Y. Sakata and S. Fukuzumi, *J. Am. Chem. Soc.*, 2001, **123**, 6617.
24 S. Fukuzumi, K. Okamoto, C. P. Gros and R. Guilard, *J. Am. Chem. Soc.*, 2004, **126**, 10441.
25 R. A. Marcus and N. Sutin, *Biochim. Biophys. Acta*, 1985, **811**, 265.
26 S. Fukuzumi, K. Ohkubo, H. Imahori, J. Shao, Z. Ou, G. Zheng, Y. Chen, R. K. Pandey, M. Fujitsuka, O. Ito and K. M. Kadish, *J. Am. Chem. Soc.*, 2001, **123**, 10676.
27 R. A. Marcus, *J. Chem. Phys.*, 1956, **24**, 966.

